ROYAL SOCIETY OPEN SCIENCE

royalsocietypublishing.org/journal/rsos

Research

Cite this article: Dowle E, Doherty J-F, Gillum J, Schmidt-Rhaesa A, Herbison REH, Poulin R, Gemmell N. 2025 Genomic insights into kin selection and developmental conflict in co-occurring hairworm parasites. *R. Soc. Open Sci.* **12**: 251698.
https://doi.org/10.1098/rsos.251698

Received: 5 September 2025
Accepted: 7 November 2025

Subject Category:
Organismal and evolutionary biology

Subject Areas:
evolution, genomics

Keywords:
parasite interactions, nematomorpha, kin selection, genome sequencing, host manipulations

Author for correspondence:
Eddy Dowle
e-mails: eddy.dowle@otago.ac.nz; eddy.dowle@plantandfood.co.nz

Genomic insights into kin selection and developmental conflict in co-occurring hairworm parasites

Eddy Dowle[1,3], Jean-François Doherty[4], Joanne Gillum[1], Andreas Schmidt-Rhaesa[5], Ryan Edward Harper Herbison[2], Robert Poulin[2] and Neil Gemmell[1]

[1]Department of Anatomy, and [2]Department of Zoology, University of Otago, Dunedin, Otago, New Zealand
[3]Plant and Food Research Group, The New Zealand Institute of Bioeconomy Science Limited, Lincoln, New Zealand
[4]Department of Zoology, Michael Smith Laboratories, Department of Biochemistry & Molecular Biology, The University of British Columbia, Vancouver, British Columbia, Canada
[5]Leibniz Institute for the Analysis of Biodiversity Change, Museum of Nature Hamburg, Hamburg, Germany

ED, 0000-0003-2265-6281; J-FD, 0000-0003-4766-9417; REHH, 0000-0001-5335-2382; RP, 0000-0003-1390-1206; NG, 0000-0003-0671-3637

Many parasites manipulate the behaviour or appearance of their host to improve their own survival or transmission, with manipulation timing tightly linked to a parasite's developmental stage. However, host manipulations are complicated by the presence of co-occurring parasites within the same host. Conspecific co-occurring parasites of similar developmental stages may interact collaboratively to manipulate a host. However, co-occurring parasites of different developmental stages will conflict with one another, especially when the manipulation is fatal to developmentally immature co-occurring parasites. Kin selection further complicates these interactions by predicting that closely related co-occurring parasites may not interfere with the other's manipulation. Co-occurring hairworm (Nematomorpha) parasites are common, and the water-seeking manipulation mature worms induce is probably lethal to co-occurring juvenile worms. To understand the role that kin selection may have on these interactions, we assess kin relationships in a wild hairworm population. We sequence, to our knowledge the first, New Zealand hairworm (*Gordius paranensis*) genome and use reduced representation sequencing to estimate relatedness among

THE ROYAL SOCIETY PUBLISHING

co-occurring worms. We show that co-occurring hairworm relatedness varies from unrelated to highly related and that both mature and immature worms inhabit the same host. We discuss how these developmental and kinship dynamics may shape host manipulations and hairworm survival.

1. Introduction

Nematomorpha or hairworms are an entirely parasitic phylum that infect arthropods [1]. Their complicated life history involves passing between two hosts and moving from freshwater to a terrestrial environment and back again [1–3]. The movement from a terrestrial to a freshwater environment is accomplished by a manipulation of the terrestrial arthropod host to enter water [3]. This has led to them being touted as a classic example of host manipulation or extended phenotype [4], where the genes of the parasite alter the phenotype of the host [5]. Though not nearly as extreme as at times suggested in the literature [6], research does suggest that terrestrial insect hosts can be manipulated to enter water to facilitate the transfer of the parasite to the freshwater environment [7–10]. Little genomic work has been conducted on this phylum, and worm development, including the mechanism of the extended phenotype, is not well understood.

However, manipulation of the host may not simply involve a fully developed worm initiating a phenotype change. Co-occurring conspecific hairworm infections, i.e. the presence of more than one worm in a single host, have been observed, with records of up to 12% of infections involving multiple worms [11]. Co-infections by the same or different species of manipulating parasites have been documented across a range of taxa [12–14], and the limited studies in this area to date have shown that co-occurring parasitic interactions can involve various levels of collaboration or conflict [15–22]. Co-occurring parasites sharing the same host may be at different development stages, i.e. different ages, with only fully developed individuals potentially benefitting from host manipulation [15]. Conspecific interactions are further complicated by kin selection which predicts that co-occurring parasites are more likely to collaborate with close kin and conflict with non-kin [23–25]. Brown [21] developed a theoretical cost-benefit model of host manipulations with co-occurring parasites that incorporated kin selection, however, there is very little information on how naturally co-occurring conspecific parasites vary in relatedness [25,26].

Hairworms, with their commonly observed co-infections and fatal host manipulation, may provide a promising system to better understand the impacts of co-occurring parasite interactions. If worms can detect the presence of a co-occurring worm, we assume their response will probably depend on two factors: (i) age difference between the worms, and (ii) the relatedness of the worms (figure 1). Co-occurring worms of the same age, i.e. dual infections resulting from a single infection exposure, may work together to drive any host phenotypic changes (sharing the metabolic cost of driving a manipulation), or one worm may drive the host manipulation while the other assumes a passive role (avoiding the metabolic cost of the manipulation). However, co-occurring worms resulting from multiple infection exposures at different times may not be at comparable life stages. When mature and juvenile worms reside in the same host, the mature worm manipulating the host to enter water is probably lethal to any co-occurring immature worms. Though laboratory studies have shown hosts do not always die upon emergence [27], it has been observed that hosts may be eaten upon entering the water [9,28], suggesting that their survival post-manipulation in the wild is probably low. However, the fatal conflict between worms is further complicated by the potential role of kin selection. If the worms can detect kin, as has been shown in some nematodes [29,30], the immature worm may not attempt to sabotage the mature worm's manipulation, or the mature worm may delay a host manipulation until the close kin immature worm is ready.

Kin selection may play an integral role in the development of the collaborations or conflicts between co-occurring conspecific parasites. The complicated two-host life cycle (figure 2) of a hairworm means that a co-occurring infection involving different lineages in the final host could be the result of either the paratenic/aquatic host feeding on different egg clutches (becoming infected with two lineages) or the final host feeding on multiple paratenic hosts (increasing their exposure to different lineages). In either scenario, the final host is exposed to and infected with more than one lineage. Understanding how co-occurring worm relatedness varies in a natural population represents a first step in understanding whether hairworm infections can be used to better understand parasite–parasite interactions. In this study, we generated a genome for the New Zealand hairworm *Gordius paranensis* Camerano,

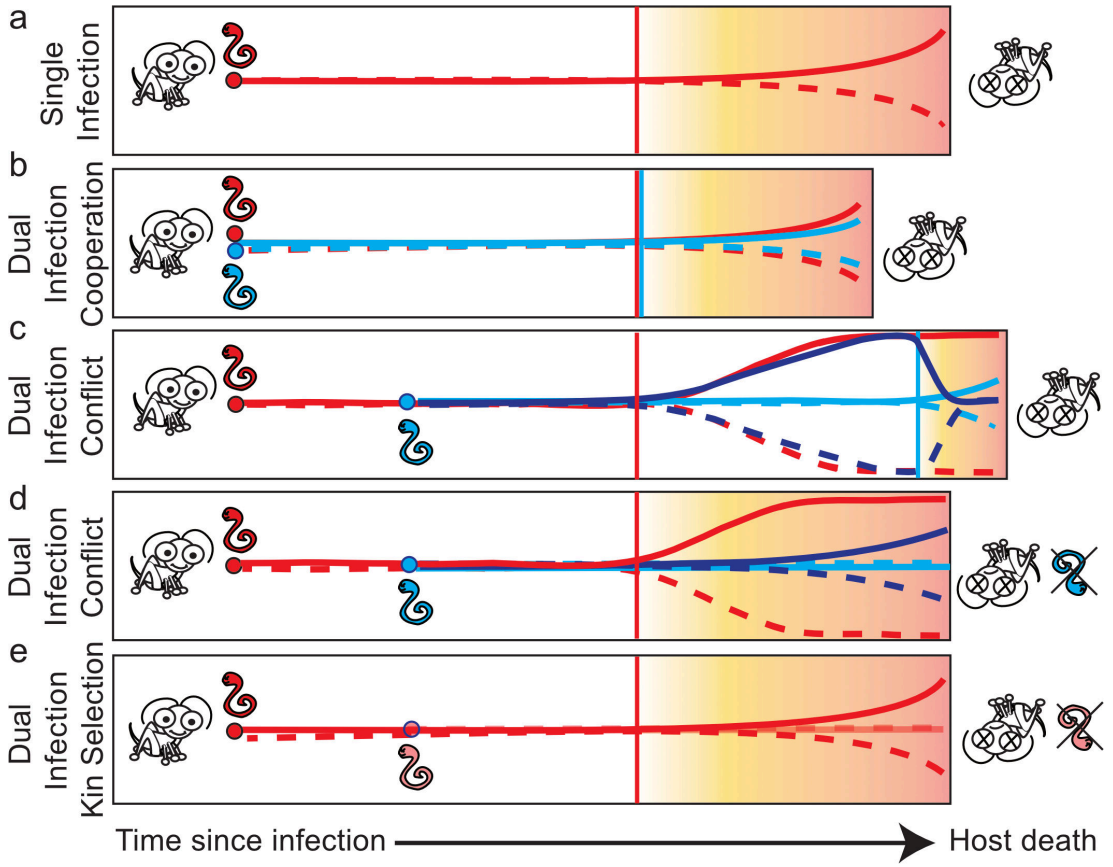

Figure 1. Overview of five possible scenarios from a dual infection. In these scenarios, worms are infected by a single (a) or dual infection (b–e). Shading to the right shows predicted host manipulation times occurring when a worm reaches maturity. Vertical red and blue lines indicate the onset of host manipulation by the worm. Horizontal lines indicate the gene expression changes in the worms associated with the manipulation. Gene expression changes in the worm probably involve both the upregulation (solid line) and downregulation (broken line) of genes. (a) Single infection worm resulting in behavioural manipulation and host death. (b) Dual infection of similar aged worms resulting in host death (in this example, both worms contribute to a host manipulation, and an alternative scenario would be for one worm to assume a passive role). (c) Dual infection of different aged worms with no kin selection (worms are in conflict); here, the immature worm delays the behavioural manipulation (gene expression changes of manipulation interference indicated with dark blue lines). (d) Dual infection of different aged worms with no kin selection (worms are in conflict); here, the immature worm fails to counter the mature worms' behavioural manipulation and dies with the host. (e) Dual infection with kin selection, here the immature worm does not attempt to counter the host manipulation and dies with the host (an alternative scenario would be for the larger worm to delay the host manipulation until the immature worm has matured).

1892. This represents one of the few genomes available for this phylum and an important genomic resource [31,32]. We then sampled a range of infected hosts and free-living worms from the same location and conducted genotype-by-sequencing (GBS) on the worms to generate kinship estimates between co-occurring worms to assess the relatedness between worms and determine what role, if any, kin selection may have in naturally co-occurring hairworm infections.

2. Methods

2.1. Sampling

Hairworms (*G. paranensis*) were collected from cave wētā (*Pleioplectron simplex*) hosts or free-living mating tangles (gordian knots) found within an adjacent stream from the Cass region of Te Waipounamu Aotearoa, South Island, New Zealand (43°02′ 3.254″ S, 171°45′ 50.612″ E; figure 3). At this location, *G. paranensis* has only been observed in tree wētā (*Hemideina* sp.) and cave wētā hosts; however, as cave wētā are easier to sample in this location, collections from live hosts were limited to cave wētā. This hairworm species has also been observed in two species of ground beetle and a wolf

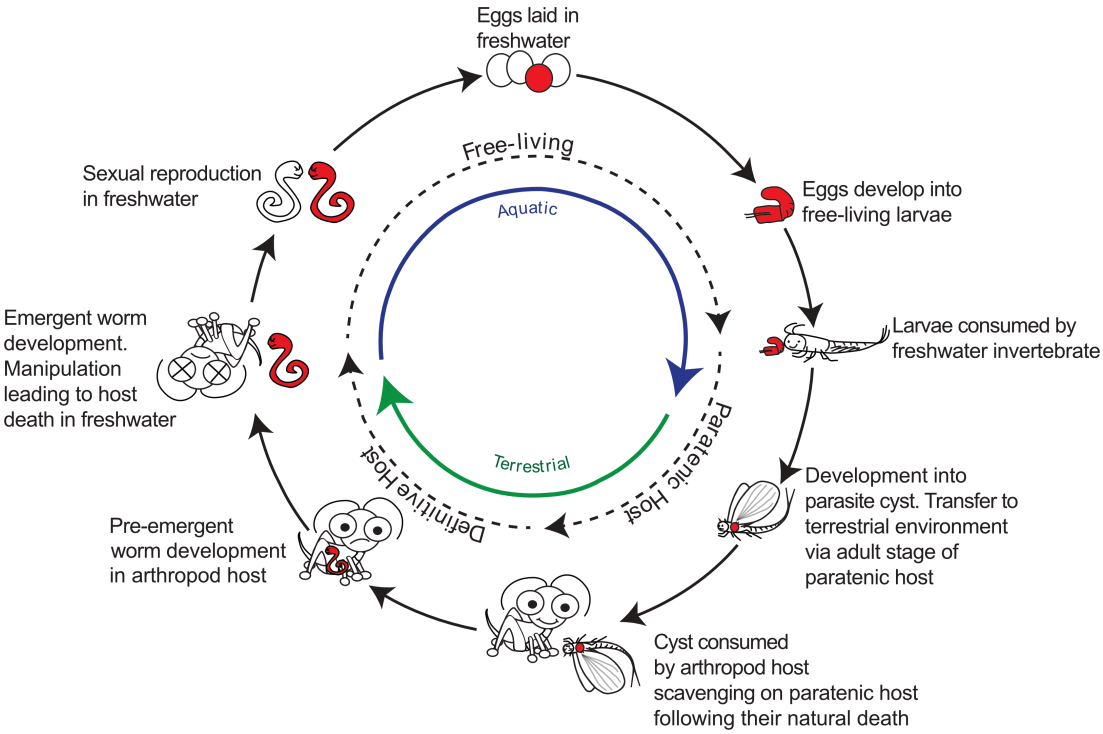

Figure 2. Overview of *Gordius paranensis* life cycle.

spider at another collection site in the South Island [11]. Adult free-living hairworms collected from the field probably represent a mix of worms from both tree and cave wētā hosts. In total, 83 hairworm samples were collected, representing an approximately 11.5% infection rate in cave wētā hosts (figure 2, overview of life cycle). Of these 83 hairworms, 56 worms were collected from within their host, and 27 free-living hairworms were collected directly from the stream (figure 3). The 56 worm samples collected directly from hosts represented 10 co-infections (ranging from 2 to 9 worms) and 13 single infections.

Samples were either frozen on site using a dry shipper or hosts were captured and returned to the laboratory. Hosts returned to the laboratory were kept in a temperature-controlled room and killed (liquid nitrogen) as part of other experiments, worms were collected either within the host during infection or at the time of emergence. Where possible, worms collected from hosts were photographed and measured; however, owing to the nature of various experiments, not all worms were measured. Dissected worms were classed as either juvenile (pale, unmelanized worms with a thin juvenile cuticle) or mature (large, melanized worms with a thick adult cuticle). Individual worms were stored at −80°C until extraction.

2.2. Species identification

Species identification was confirmed by the examination of a single male hairworm. Body sections of about 1 mm length from the middle region and the entire posterior end of one male were dehydrated in a series of increasing ethanol concentrations, critical point dried in a Leica EM CPD300 Critical Point Dryer, sputter coated with gold Sputter Coater and investigated with a LEO SEM 1524 scanning electron microscope. Identification was based on morphological characteristics, i.e. the cuticular structure and especially the presence of a semicircular row of bristles anterior to the cloacal opening, a distinguishing feature of *G. paranensis* [33].

2.3. Genome sequencing

A hybrid genome assembly was generated using 10× Genomics linked reads and Nanopore reads. A male hairworm (XY/XX system) was extracted using a Nanobind Tissue Big DNA kit (Circulomics, USA). This individual (code W136) was used for both 10× Genomic linked read library preparation

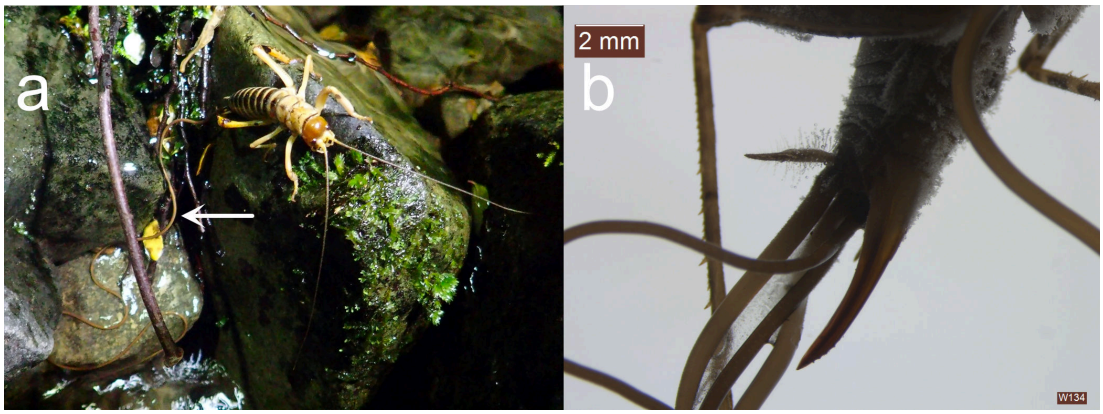

Figure 3. (a) *Gordius paranensis* emerging from a tree wētā host at Cass, New Zealand. (b) Emergence of four hairworms from a single cave wētā host. Photo credits: Jean-François Doherty.

and Nanopore long-read sequencing. Linked read libraries were prepared as per the manufacturer's instructions. Briefly, DNA samples underwent an RNase A treatment before quantification on a Qubit 2.0 fluorometer. DNA was then size selected for fragments over 40 kbp using a BluePippin (Sage Science, USA), and a 10× Chromium linked read (10× Genomics, USA) library was prepared following the 10× Genomics linked read's instructions. The library was sequenced on the Illumina NovaSeq 6000 platform for 2 × 150 bp reads at the Garvan Institute, Australia.

Long-read sequencing libraries for Oxford nanopore sequencing were prepared using 3000 ng of total DNA per run with the SQK-LSK109 ligation sequencing kit (Oxford Nanopore Technologies, Oxford, UK) following the manufacturer's instructions. The prepared libraries were sequenced using two R9 MinION flow cells (FLO-MIN106) run for 72 h.

2.4. RNA sequencing transcriptome

To improve the annotation quality of the genome, RNA was extracted from five worms (codes W3_small (unsexed), W3_large (unsexed, juvenile), W32 (unsexed, juvenile), W35 (unsexed, juvenile) and W134_worm2 (female mature)) using a Direct-zol RNA miniprep kit (Zymo) with on-column DNase-1 treatment to profile the transcriptome. RNA quality and quantity were assessed using a Bioanalyser and Qubit. Samples were prepared at the Otago Genomics Facility (New Zealand) using a TruSeq Illumina Stranded messenger RNA (mRNA) kit and sequenced for 2 × 100 bp reads on an Illumina Hiseq 2000.

2.5. Reduced representation sequencing

We assessed the relationship between co-occurring hairworms using a reduced representation sequencing approach, GBS. A total of 56 worms were sequenced using a GBS approach from the single Cass population; owing to difficulties in extracting high-quality DNA, not all available worms were successfully extracted and sequenced. Of the 56 worms sequenced, 30 were from co-infections (each contained 2–9 worms); these represented nine total co-infected hosts, and the rest comprised single infection worms (10 total) or free-living hairworms sampled outside of a host (16 worms). DNA was extracted using a lithium chloride and chloroform salting-out method [34]. DNA quality and quantity were checked post-extraction using agarose gel electrophoresis, Denovix and Qubit. For many of the worms, a limited amount of DNA was available (e.g. <10 ng ul^{-1}) and to meet the requirements for GBS sequencing (30 µl at 20 ng $µl^{-1}$), 19 samples were amplified using REPLI-g Mini Kit (Qiagen) as per the manufacturer's instructions. To confirm the presence of a single species, a 255 bp fragment of cytochrome c oxidase subunit I (COI) was amplified using the hairworm COI primers developed by [35] and a neighbour-joining tree with hairworm sequences downloaded from The National Center for Biotechnology Information (NCBI) [36] was generated in Geneious Prime v. 2024.0.5. This confirmed the presence of a single monophyletic cluster of sequences sister to previously sequenced *G. paraenesis* species from New Zealand (KY172753-6, KY172776, KY172782, KY172811-3) and 12 other undescribed *Gordius* sp. sequences. The successful 56 extractions were then sent for GBS library preparation using

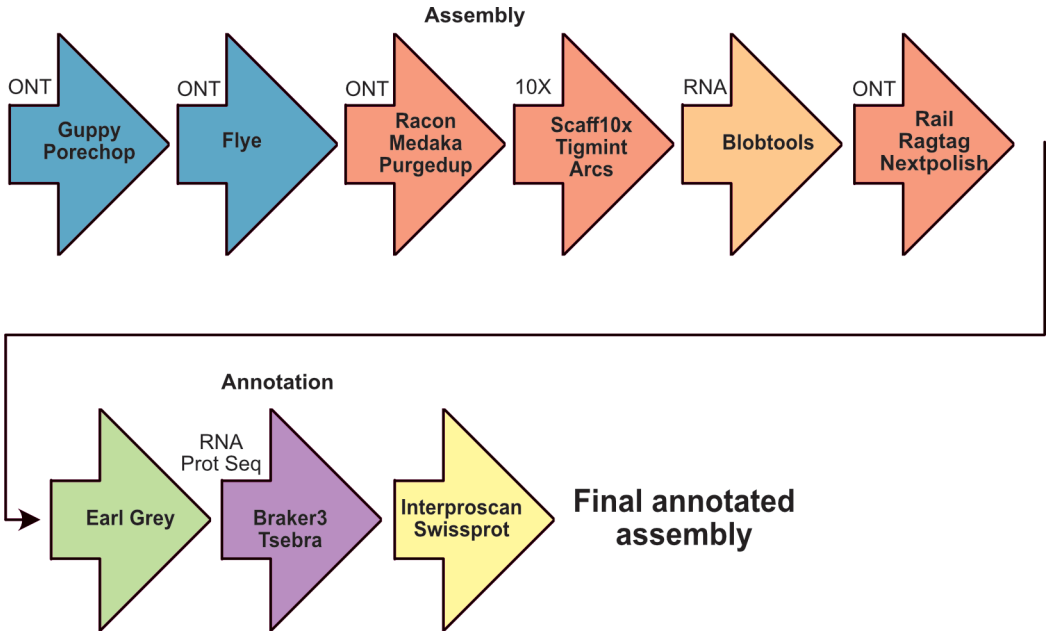

Figure 4. Overview of the steps undertaken to generate the final annotated assembly, including initial sequencing and assembly (blue), scaffolding and polishing (red), decontamination (orange), repeat masking (green), annotation (purple) and functional annotation (yellow). Data used are indicated above the arrow as either Oxford Nanopore Technologies (ONT, long reads), 10× (linked reads), RNA (mRNA sequence reads) or Prot Seq (protein sequences downloaded from NCBI).

the restriction enzymes *APe*KI and *Msp*I and sequencing across a NovaSeq for 1 × 100 single ended reads at AgResearch (Invermay, Dunedin).

2.6. Genome assembly

The genome assembly is available from NCBI JBMBTH000000000. To ascertain the most appropriate method of combining the two sequencing approaches (10× Genomics linked reads and Nanopore long reads), two draft assemblies were generated, a Supernova v. 2.1.1 [37] assembly from linked reads and a Flye v. 2.9.1 [38] assembly from the long reads, and compared using BUSCO (implemented via compleasm v. 0.2.5) [39,40] and QUAST v. 5.2.0 [41]. Owing to the higher quality of the initial Flye assembly, we used the long reads to generate our base assembly with the linked reads used for scaffolding at later steps (figure 4). An estimate of the genome size was undertaken using the forward linked read; the read was trimmed using Trimmomatic v. 0.38 [42] to remove TruSeq adapters, 10× Genomics adapters (first 16 bp), low-quality reads (sliding windows 2:30:10) and reads less than 35 bp long. A histogram of kmers was generated using KMC v. 3.1.1 [43] with a kmer length of 21, before the resulting histogram was visualized in GenomeScope v. 2.0 [44] online.

All long reads were base-called using Guppy v. 6.2.1 (Nanopore), with summary statistics generated using pycoQC v. 2.5.2 [45], before adapters were trimmed using Porechop v. 0.2.4 (github.com/rrwick/Porechop). A draft assembly was then built using Flye v. 2.9.1 [38] and polished using four rounds of Racon v. 1.4.3 (github.com/isovic/racon) and one round of medaka2 (github.com/nanoporetech/medaka) using the raw long reads. Duplicate haplotigs were then removed using Purgehaplotigs v. 1.2.5 [46] before linked reads exported using Longranger basic v. 2.2.2 (10× Genomics) were used to scaffold the genome using Scaff10× v. 4.2 (github.com/wtsi-hpag/Scaff10X) and Tigmint and Arks v. 1.2.8 [47]. The draft assembly was then cleaned to remove scaffolds less than 50 bp, before the RNA sequencing data were mapped to it using STAR v. 2.7.10 [48], and BlobTools2 v. 4.1.5 [49] was used to identify and remove scaffolds that did not hit any of the available sequences for Nematomorpha on NCBI and had no RNA sequencing mapping consistent with gene regions (e.g. contigs with no hits to Nematomorpha and only homopolymer mapping were excluded). The cleaned genome underwent a final round of long-read scaffolding using Rails v. 1.5.1 [50] and Ragtag v. 2.1.0 [51] before a final round of

error correction using the long-read polisher NextPolish v. 1.4.0 (github.com/Nextomics/NextPolish).

2.7. Genome annotation

Before annotation, repetitive content was annotated using the Earl Grey pipeline 4.1.0 [52] and a soft-masked genome was generated. Protein gene annotation was undertaken in Braker3 v. 3.0.3 [53] using both protein and RNA sequencing hints. Reference protein sequences comprised both the OrthoDB 11 Metazoan database (as recommended by Braker and Prothint v. 2.6.0 (github.com/gatech-genemark/ProtHint)) and available Nematomorpha protein sequences from the species *Gordionus montsenyensis* and were pre-processed for Braker3 using Prothint. RNA sequencing hints solely comprised those reads generated in this study for *G. paranensis*. Following Braker3, TSEBRA v. 1.1.2 [54] was rerun using the Augustus [55] and Braker hints file, and a final gtf and protein prediction file were generated. Functional annotation of predicted genes was assessed using InterProScan v. 5.64 (github.com/ebi-pf-team/interproscan) with both mappings to gene ontology terms and MetaCyc and Reactome pathways (option -goterms and -pathways) and blastp v. 2.16 [56] (e-value threshold 1×10^{-6}) of protein sequences to the SwissProt database. Functional annotations were merged into the gff file (agat_sp_manage_functional_annotation.pl) and summary statistics (agat_sq_stat_basic.pl) generated using AGAT v. 1.0 (github.com/NBISweden/AGAT). To understand the completeness of the profiled transcriptome, a de novo transcriptome assembly was generated using Trinity v. 2.14.0 [57] and assessed using BUSCO v. 5.6.1 [39].

2.8. Kinship analysis of genotype-by-sequencing data

To generate King, R0 and R1 estimates of the relationship, GBS samples were demultiplexed using the process_radtags v. 2.65 script from STACKS2 [58] before reads were mapped to the assembled genome using BWA v. 0.7.17 [59]. Bam mapping files were then used as inputs into ANGSD v. 9.4 [60] to generate an allele frequency input file for NgsRelate v. 2 [61]. Kinship values generated in NgsRelate and KING-robust estimates plotted for pairs with more than 400 single nucleotide polymorphism (SNP) sites in R v. 4.4.1 [62]. KING-robust relationship inference estimates are applicable to samples from the same population when allele frequencies are unknown and can be used to infer if individuals are parent–offspring, full-sibling, half-sibling/grandparent–grandchild, first cousin or unrelated [62].

3. Results

3.1. Genome and transcriptome assembly

The haploid genome size estimate based on the forward-linked read in genome scope was 143.942 Mb (min) to 152.297 Mb (max) with a heterozygosity level of 5.44% (min) to 5.68% (max). A total of more than 123 million paired-end 10× linked reads were generated. Supernova estimated a genome size of 360 Mb, and the draft Supernova assembly (input reads down-sampled to 56× coverage) had a total length of 205 Mb across 16 942 scaffolds, with an N50 of 39 790, and L50 of 1376 (table 1). Compleasm reported a complete BUSCO score of 67% and a partial BUSCO score of 8% using the Metazoa OB10 database.

The long-read sequencing yielded >11.67 Gb of passing (as called in Guppy, approx. 14.5 Gb raw data) data across two Nanopore minion flow cells. The median passing read length and PHRED score were 1240 bp and 11.7, respectively. Flye generated a draft assembly of 244 Mb, across 14 095 contigs, with an N50 of 1 493 312 and L50 of 361. Compleasm reported a complete BUSCO score of 72% and a partial BUSCO score of 3% using the Metazoan OBD10 database. The long-read assembly was more complete with better contiguity than the draft linked-read assembly (table 1). As such, this assembly underwent further scaffolding, correcting and cleaning using both the long reads and linked reads to generate a final assembly (figure 4).

The final assembly had a length of 164.051 Mb, similar to the genome scope estimate of 143–152 Mb, across 360 scaffolds with an L50 of 40 (table 1). The compleasm BUSCO score to the Eukaryote database was 87% complete, with a further 3.9% fragmented. This suggests that despite the extremely high levels of estimated heterozygosity, the final genome is relatively complete and contiguous.

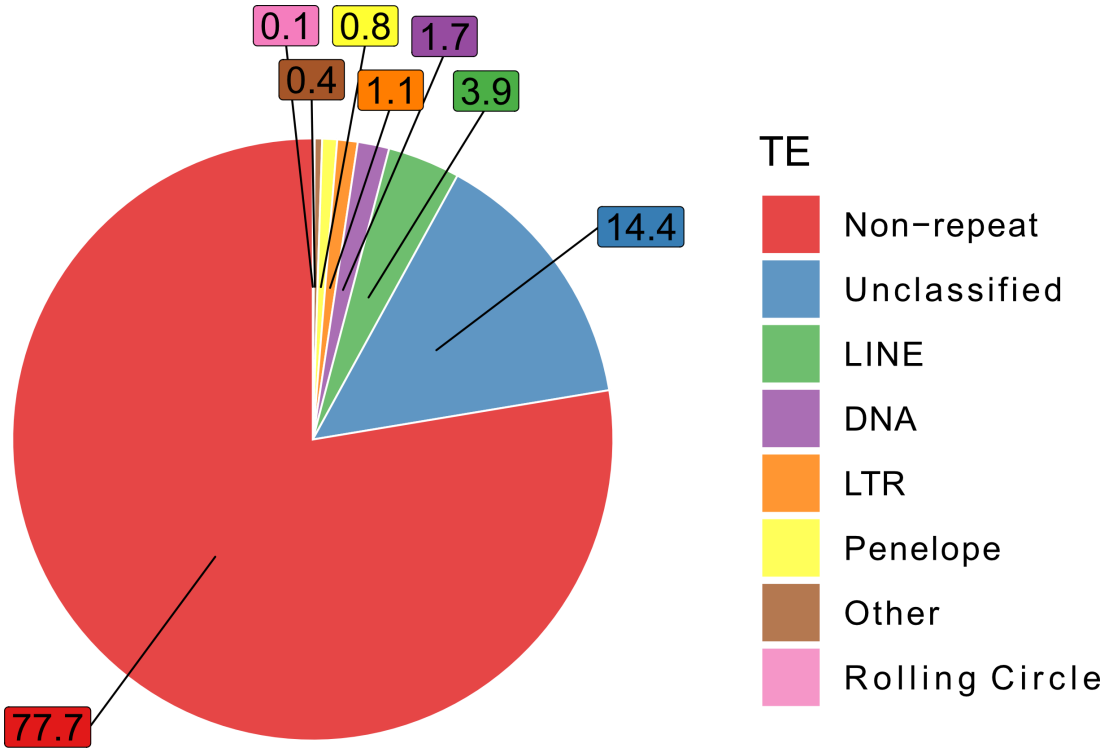

Figure 5. Summary of the repeats annotated through the Earl Grey pipeline. The 'other' category comprised simple, microsatellite and RNA repeats.

Table 1. Assembly statistics from the draft linked read (10× Genomics) and long-read (Nanopore) assemblies, along with the final assembly. (BUSCO scores were estimated in compleasm using the eukaryote (BUSCO E %) and metazoan (BUSCO M %) database.)

assembly	length (Mb)	no. scaffolds	GC%	N50	L50	Ns per 100 kbp	BUSCO E % compleasm	BUSCO M % compleasm
raw linked read assembly	214.812	16 942	31.06	39 790	1376	1,415.7	61.18 (s)	54.30 (c)
							14.90 (d)	12.68 (d)
							14.51(f)	8.07 (f)
raw long-read assembly	253.382	14 095	30.89	1 49 312	361	0.00	72.94 (s)	63.00 (c)
							12.55 (d)	9.33 (d)
							4.71(f)	3.35 (f)
final assembly	164.051	360	31.02	1,137,137	40	0.00	85.5% (c)	71.17 (c)
							1.57 (d)	0.63 (d)
							3.9% (f)	3.25 (f)

3.2. Genome annotation

Transposable elements (TEs) identified using the Earl Grey pipeline [52] comprised 22.3% of the genome (figure 5). These largely comprised unclassified TEs (14.4%), long interspersed nuclear elements (LINE) (3.9%), DNA (1.7%) and long terminal repeats (LTR) (1%).

For genome annotation, more than 2.1 Gb of short-read Illumina RNA sequencing data were generated from profiling the transcriptome of immature *G. paranensis* worms. The de novo transcriptome assembly generated using Trinity suggested that the profiled transcriptome was missing some genes (13.6% of metazoan BUSCO genes were missing); this probably would have been improved by the inclusion of other life stages (e.g. larval, early and mature free-living worms). In total, 15 272 836 metazoan and Nematomorpha protein sequences were downloaded, prepared in Prothint and run alongside the RNA sequencing data as hints in Braker3. Annotation in Braker3 resulted in 10 646 genes predicted with an average of 7.7 exons per transcript. BUSCO analysis on the predicted genes

Table 2. Final assembly statistics. (Transcriptome and annotation BUSCO completeness scores were generated using the Eukaryote and Metazoa OB10 database. Gene and annotation statistics were generated using AGAT.)

statistic	assembly
RNA-seq produced transcriptome (BUSCO)	**de novo transcriptome (Trinity)**
BUSCO (transcriptome: Eukaryote)	N:255 (genes checked)
complete single	45.5% (N:116)
complete duplicated	35.3% (N:90)
fragmented	12.5% (N:32)
missing	6.7% (N:17)
BUSCO (transcriptome: Metazoa)	N:954 (genes checked)
complete single	43.4% (N:414)
complete duplicated	29.4% (N:280)
fragmented	13.6% (N:130)
missing	13.6% (N:130)
gene prediction (compleasm)	**final assembly**
BUSCO (Eukaryote_obd10)	N:255 (genes checked)
complete single	64.3% (N:164)
complete duplicated	24.3% (N:62)
fragmented	46.3% (N:16)
missing	5.1% (N:13)
BUSCO (Metazoan_obd10)	N:954 (genes checked)
complete single	58.6% (N:559)
complete duplicated	19.6% (N:187)
fragmented	5.1% (N:49)
missing	16.7% (N:159)
genes	
total number	10 646
average length	6904 bp
mean transcripts per gene	1.2
transcripts	
total number	12 923
average length	7024 bp
mean exons per transcript	7.7
coding DNA sequence (CDS)	
total number	12 923
average length	1516 bp
exons	
total number	98 716
mean length	193 bp
gene function	
total number genes with functional annotation	9096
total number mRNA with functional annotation	11 196

was similar to that of the transcriptome complete (16.7% of metazoan BUSCO genes were missing), with 19.6% duplicated (table 2).

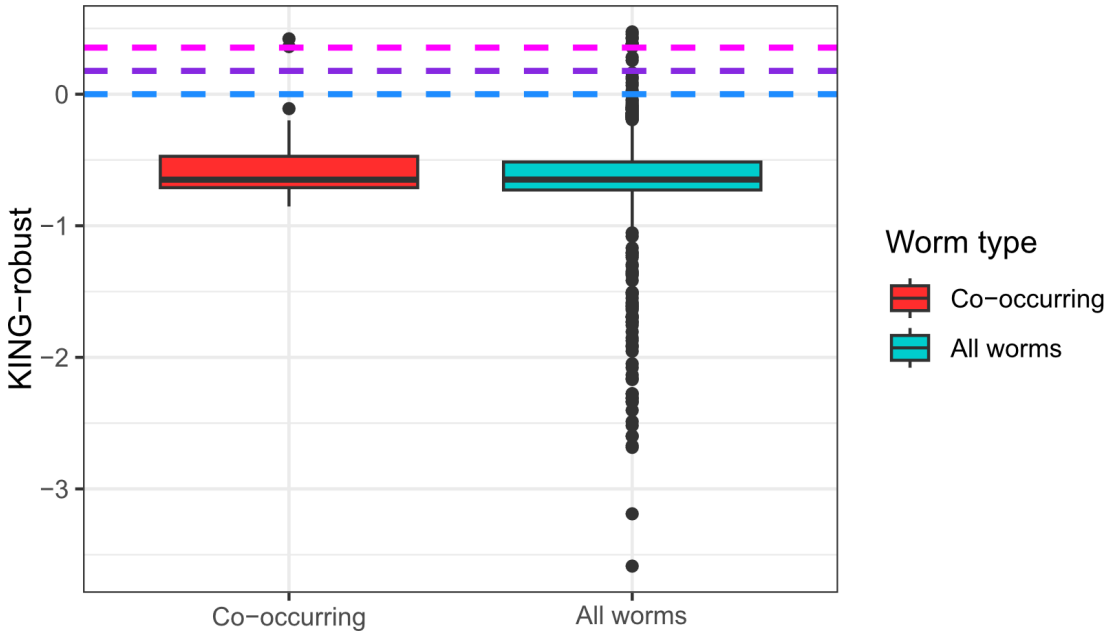

Figure 6. Relatedness estimates (KING-robust) for all worm comparisons with more than 400 SNPs in a pairwise comparison. Of the nine hosts with co-occurring worms, two hosts contained highly related worms (dots above the pink line). The remaining co-occurring worms were unrelated (below the blue line). Dashed lines represent the theoretical limits for familial relationships in KING-robust kinship, based on large, outbred populations (below blue = unrelated, purple = half-siblings, pink = full siblings).

3.3. Kinship estimates

Over the course of this study, 23 infected cave wētā hosts were collected, of which 10 had co-occurring parasite infections, suggesting co-infection is common. In total, 56 worms, including representatives from nine co-infections, had enough DNA for GBS. Samples had an average sequence read count passing filter of 5 413 098. Kinship was estimated from only mapped reads, with mapping rates averaging 44% to the assembled genome. Blasting of unmapped reads suggested that the lower-than-expected mapping rate was a result of host and bacterial contamination, the latter of which was probably exacerbated by the use of whole genome amplification prior to library preparation [63]. To understand how relatedness varied in co-occurring worms, KING-robust estimates were generated in NgsRelate. Relatedness estimates across all the worms varied from unrelated to highly related (KING estimates >0.354, which in a large, outbred population is a theoretical limit for a monozygotic twin). Of the nine hosts with co-occurring worms sequenced, two hosts contained worms that were highly related (KING >0.25), the rest contained unrelated worms (figure 6).

3.4. Size variation

Worm size varied from 6 to 449 mm for all worms and 64–449 mm for mature free-living worms and mature dissected worms (large worms with brown cuticle pigmentation; figure 3). It was not possible to determine the host of worms caught free living, however, some probably emerged from larger tree wētā hosts (approx. 10 times heavier than *P. simplex* cave wētā). From the worms dissected from cave wētā, nine were classified as mature worms (large worms with brown cuticle pigmentation) and 21 were classified as juvenile (white in appearance) (figure 7). Juvenile worms were generally smaller than adult worms, suggesting that size is a proxy for age. Within the worms dissected from the nine hosts with co-occurring parasites, the ratio of worm sizes ranges from 0.06 to 0.99 (table 3). Both highly related co-occurring parasites were of a similar size (ratios of 0.84 and 0.99), while unrelated co-occurring parasites ranged from highly dissimilar ratios (0.06) to very similar ratios (0.97).

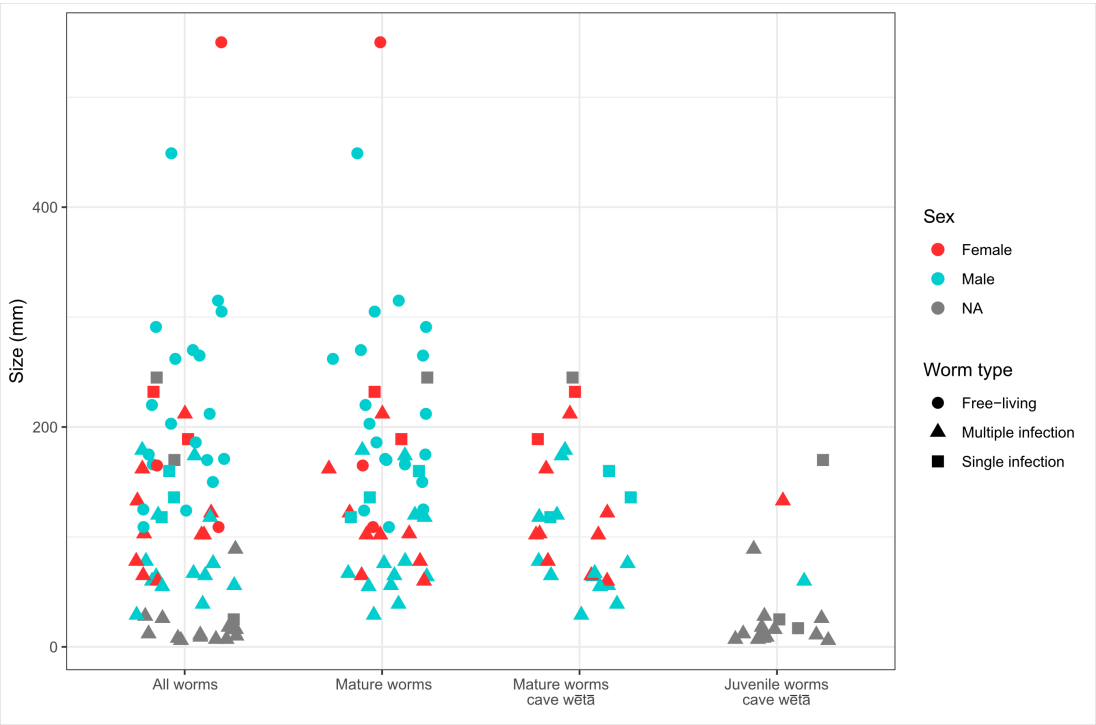

Figure 7. Size ranges of *Gordius parenensis* collected from Cass. Not all worms were able to be sexed, and 'all worms' probably represent worms from a mix of both tree and cave wētā hosts.

Table 3. Information on co-occurring worms that underwent sequencing (GBS). (Owing to the challenges associated with extracting high-quality DNA from hairworms, not all were successfully sequenced. Numbers reflect the sequenced worms with the values for all worms present in a host (regardless of successful sequencing) indicated within the brackets.)

wētā individual	number of worms sequenced (number present)	sequenced worm ages (present worm ages)	sequenced worm size range mm (present worm range)	maximum size ratio variation (present worm maximum ratio)	KING-robust estimates
W58	8 (13)	juvenile	7–89 (6–89)	0.08 (0.07)	<0
W133	2 (3)	mature (juvenile)	102–103 (60–103)	0.99 (0.58)	0.42
W134	2 (4)	mature	102–122 (64–122)	0.84 (0.52)	0.36
W138	2 (2)	mature + juvenile	120–133	0.9	<0
14	7 (9)	NA	29–118 (29–118)	0.25 (0.25)	<0
17	2 (2)	NA	76–78	0.97	<0
24	2 (2)	NA	162–212	0.76	<0
29	2 (2)	NA	174–179	0.97	<0
Ch11	3 (4)	juvenile (mature)	NA		<0

4. Discussion

Hairworms (Nematomorpha) have been largely understudied genetically despite their fascinating life history [31,32]. Here, we add to the sparse genomic resources for this phylum with a relatively draft genome for the New Zealand species *G. paranensis*.

Cunha *et al*. [31] found that the genome assemblies of *Acutogordius australiensis* and *Nectonema munidae* had a rampant loss of universal metazoan genes as determined by BUSCO scores. Here, we report a complete and fragmented score against the metazoan gene set of 75% (missing 25%), somewhat higher than the values reported for the available genomes (67–73%). However, our predicted

gene set had a far lower missing rate of 16.7% and the profiled transcriptome was missing even less (13.6%) despite using only one life stage. Given that the genome is not at the chromosome level and improvements in assembly and annotation will improve gene annotation, it is unlikely that the rampant loss of universal metazoan genes noted in other hairworm genomes is universal across the phylum. Detailed comparative analyses using a broader range of Nematomorpha genomes are needed to better understand the evolution of this phylum.

Co-infections (i.e. two or more parasites sharing the same individual host) are common in parasites, but their implications for parasite manipulation are not well studied [12–14,20]. In hairworms, co-infections will impact both worm development via competition for resources and, if the development stage differs, the timing of host manipulation (and resulting host death), which would be lethal to undeveloped co-occurring parasites. Understanding how relatedness and development vary between wild co-occurring hairworms is a crucial step to evaluating whether hairworms represent a good model of parasite co-infection. Of the 23 hosts collected throughout the course of this study, 10 were co-infected. It is not clear what co-infection rates are in other hairworm species, but with a co-infection rate of almost 50% at this sampling location, *G. paranensis* represents a useful study system to better understand conspecific co-occurring parasite infections.

Kin selection has been shown to be a factor in co-occurring parasite interactions [25,26]. Our results are limited by our small sample size that reflects the difficulty of sampling large numbers of infected hosts from the wild; nevertheless, relatedness varied between co-occurring worms. Though not significant, we found co-occurring unrelated worms to be more common than co-occurring related worms (seven out of nine cases). Co-occurring unrelated worms ranged from similar sizes to highly different sizes, suggesting that infections by unrelated worms probably represented hosts co-infected from both a single infection event (consumption of a single paratenic host infected by several worm lineages) and hosts co-infected from multiple infection events. The two infections of highly related worms comprised worms of similar sizes, suggesting that they probably represented one infection event, perhaps occurring from the wētā host feeding on a single paratenic host that was infected with closely related larval worms. If most kin infections occur from a single infection event and reach maturity at a similar time, kin selection may not contribute significantly to co-occurring hairworm interactions. Though collaboration to induce host manipulation would reduce the individual metabolic cost incurred by each worm, a lack of collaboration may enable the passive worm to avoid any metabolic cost associated with manipulation. However, our sample size (only two cases) is too low to conclude that these relationships always involve worms of a similar age.

Co-occurring parasites of different development stages are likely to be in conflict with each other when the older reaches the final stages of infection (figure 1). These conflicts could lower the fitness of worms forced to emerge too early and worms forced to delay their emergence (emerging too late). Host manipulation timing and worm maturity have been tightly linked to worm fecundity, with an over threefold decrease in fecundity in worms emerging too early or too late [10]. Several of the co-occurring worms in this study are likely to be in conflict with one another. For example, two hosts harboured worms with highly different sizes (likely to result in a mismatching of manipulation timing), and despite having worms of similar sizes (size ratio of 0.9), host W138 harboured both a mature and an immature worm. Further work is needed to determine whether co-occurring hairworms can not only detect one another within a host but also distinguish kin from non-kin. Nevertheless, despite the limitations of this study, many co-occurring worms appear to be in clear and direct conflict of interest regarding the timing of host manipulation.

5. Conclusion

It is unknown whether hairworms can strategically adjust their strategy to either collaborate in the manipulation effort or thwart the manipulation effort of a co-infecting worm. However, the high rates of co-infections and varying levels of relatedness and maturity between co-occurring worms uncovered here, along with previous work highlighting the impacts of worm maturity on fecundity [10], suggest there would be advantages to worms capable of interfering with one another's host manipulation. Studies, such as this one, from wild systems are important to show how co-occurring worm relatedness naturally varies. However, given the low infection rates (approx. 11.5% of which 50% have co-occurring worms), further behavioural and genomic work using laboratory infections of single and dual parasite infection exposures with unrelated and related worms would be needed to fully understand how co-occurring hairworms interact with one another inside a host. Hairworm species can be used in

controlled laboratory infection trials [64], and they represent a promising system to better understand conspecific parasite–parasite interactions.

Ethics. The genome was published following consultation with Arowhenua rūnanga. Collections occurred with permission of the land owners, and invertebrates are not covered under the animal ethics committee.

Data accessibility. Raw reads are available from NCBI project code: PRJNA1234713. Genome ID JBMBTH000000000, and scripts for all analyses are available from [65]. Genome annotations are available from Dryad [66].

Declaration of AI use. We used AI-assisted technologies for grammar checking.

Authors' contributions. E.D.: conceptualization, data curation, formal analysis, funding acquisition, investigation, methodology, project administration, validation, visualization, writing—original draft, writing—review and editing; J.-F.D.: data curation, writing—review and editing; J.G.: data curation, investigation, methodology, writing—review and editing; A.S.-R.: formal analysis, methodology, writing—review and editing; R.E.H.H.: methodology, writing—review and editing; R.P.: conceptualization, funding acquisition, project administration, supervision, writing—review and editing; N.G.: conceptualization, funding acquisition, project administration, resources, supervision, writing—review and editing.

All authors gave final approval for publication and agreed to be held accountable for the work performed therein.

Conflict of interest declaration. We declare we have no competing interests.

Funding. This work was funded by a Royal Society of New Zealand Marsden Fast-Start Grant (PAF1901).

References

1. Hanelt B, Thomas F, Schmidt-Rhaesa A. 2005 Biology of the phylum Nematomorpha. In *Advances in parasitology* (eds JR Baker, R Muller, D Rollinson), pp. 243–305. London, UK: Academic Press. (doi:10.1016/S0065-308X(05)59004-3)
2. Bolek MG, Schmidt-Rhaesa A, De Villalobos LC, Hanelt B. 2015 Chapter 15 - Phylum Nematomorpha. In *Thorp and Covich's freshwater invertebrates* (eds JH Thorp, DC Rogers), pp. 303–326, 4th edn. Boston, MA: Academic Press. (doi:10.1016/B978-0-12-385024-9.00010-1)
3. Hanelt B, Janovy J. 1999 The life cycle of a horsehair worm, *Gordius robustus* (Nematomorpha: Gordioidea). *J. Parasitol*. **85**, 139–141.
4. Dawkins R. 1982 *The extended phenotype*. Oxford, UK: Oxford University Press.
5. Hughes DP. 2014 On the origins of parasite-extended phenotypes. *Integr. Comp. Biol*. **54**, 210–217. (doi:10.1093/icb/icu079)
6. Doherty JF. 2020 When fiction becomes fact: exaggerating host manipulation by parasites. *Proc. R. Soc. B* **287**, 20201081. (doi:10.1098/rspb.2020.1081)
7. Thomas F, Schmidt-Rhaesa A, Martin G, Manu C, Durand P, Renaud F. 2002 Do hairworms (Nematomorpha) manipulate the water seeking behaviour of their terrestrial hosts? *J. Evol. Biol*. **15**, 356–361. (doi:10.1046/j.1420-9101.2002.00410.x)
8. Obayashi N, Iwatani Y, Sakura M, Tamotsu S, Chiu MC, Sato T. 2021 Enhanced polarotaxis can explain water-entry behaviour of mantids infected with nematomorph parasites. *Curr. Biol*. **31**, R777–R778. (doi:10.1016/j.cub.2021.05.001)
9. Sato T, Watanabe K, Kanaiwa M, Niizuma Y, Harada Y, Lafferty KD. 2011 Nematomorph parasites drive energy flow through a riparian ecosystem. *Ecology* **92**, 201–207. (doi:10.1890/09-1565.1)
10. Sanchez MI, Ponton F, Schmidt-Rhaesa A, Hughes DP, Misse D, Thomas F. 2008 Two steps to suicide in crickets harbouring hairworms. *Anim. Behav*. **76**, 1621–1624. (doi:10.1016/j.anbehav.2008.07.018)
11. Doherty JF, Filion A, Poulin R. 2022 Infection patterns and new definitive host records for New Zealand gordiid hairworms (phylum Nematomorpha). *Parasitol. Int*. **90**, 102598. (doi:10.1016/j.parint.2022.102598)
12. Cézilly F, Perrot-Minnot MJ, Rigaud T. 2014 Cooperation and conflict in host manipulation: interactions among macro-parasites and micro-organisms. *Front. Microbiol*. **5**, 248. (doi:10.3389/fmicb.2014.00248)
13. Hafer N. 2016 Conflicts over host manipulation between different parasites and pathogens: investigating the ecological and medical consequences. *BioEssays* **38**, 1027–1037. (doi:10.1002/bies.201600060)
14. Hafer N, Milinski M. 2015 Cooperation or conflict: host manipulation in multiple infections. In *Host manipulations by parasites and viruses*, pp. 49–68. Cham, Switzerland: Springer. (doi:10.1007/978-3-319-22936-2_4)
15. Dianne L, Rigaud T, Léger E, Motreuil S, Bauer A, Perrot-Minnot MJ. 2010 Intraspecific conflict over host manipulation between different larval stages of an acanthocephalan parasite. *J. Evol. Biol*. **23**, 2648–2655. (doi:10.1111/j.1420-9101.2010.02137.x)
16. Cezilly F, Gregoire A, Bertin A. 2000 Conflict between co-occurring manipulative parasites? An experimental study of the joint influence of two acanthocephalan parasites on the behaviour of *Gammarus pulex*. *Parasitology* **120**, 625–630. (doi:10.1017/s0031182099005910)
17. Sparkes TC, Wright VM, Renwick DT, Weil KA, Talkington JA, Milhalyov M. 2004 Intra-specific host sharing in the manipulative parasite *Acanthocephalus dirus* : does conflict occur over host modification? *Parasitology* **129**, 335–340. (doi:10.1017/s0031182004005645)
18. Hellard E, Fouchet D, Vavre F, Pontier D. 2015 Parasite–parasite interactions in the wild: how to detect them? *Trends Parasitol*. **31**, 640–652. (doi:10.1016/j.pt.2015.07.005)
19. Hafer N, Milinski M. 2015 When parasites disagree: evidence for parasite-induced sabotage of host manipulation. *Evolution* **69**, 611–620. (doi:10.1111/evo.12612)

20. Hafer N, Milinski M. 2016 Inter- and intraspecific conflicts between parasites over host manipulation. *Proc. R. Soc. B* **283**, 20152870. (doi:10.1098/rspb.2015.2870)
21. Brown SP. 1999 Cooperation and conflict in host–manipulating parasites. *Proc. R. Soc. B* **266**, 1899–1904. (doi:10.1098/rspb.1999.0864)
22. Buckling A, Brockhurst MA. 2008 Kin selection and the evolution of virulence. *Heredity* **100**, 484–488. (doi:10.1038/sj.hdy.6801093)
23. Vickery WL, Poulin R. 2010 The evolution of host manipulation by parasites: a game theory analysis. *Evol. Ecol*. **24**, 773–788. (doi:10.1007/s10682-009-9334-0)
24. Wickler W. 2010 Evolution-oriented ethology, kin selection, and altruistic parasites. *Zeitschrift Für Tierpsychologie* **42**, 206–214. (doi:10.1111/j.1439-0310.1976.tb00966.x)
25. Joannes A, Lagrue C, Poulin R, Beltran-Bech S. 2014 Effects of genetic similarity on the life-history strategy of co-infecting trematodes: are parasites capable of intrahost kin recognition? *J. Evol. Biol*. **27**, 1623–1630. (doi:10.1111/jeb.12413)
26. Criscione CD, van Paridon BJ, Gilleard JS, Goater CP. 2020 Clonemate cotransmission supports a role for kin selection in a puppeteer parasite. *Proc. Natl Acad. Sci. USA* **117**, 5970–5976. (doi:10.1073/pnas.1922272117)
27. Biron DG, Ponton F, Joly C, Menigoz A, Hanelt B, Thomas F. 2005 Water-seeking behavior in insects harboring hairworms: should the host collaborate? *Behav. Ecol*. **16**, 656–660. (doi:10.1093/beheco/ari039)
28. Ponton F, Lebarbenchon C, Lefèvre T, Biron DG, Duneau D, Hughes DP, Thomas F. 2006 Parasitology: parasite survives predation on its host. *Nature* **440**, 756–756. (doi:10.1038/440756a)
29. Hiramatsu F, Lightfoot JW. 2023 Kin-recognition and predation shape collective behaviors in the cannibalistic nematode *Pristionchus pacificus*. *PLoS Genet*. **19**, e1011056. (doi:10.1371/journal.pgen.1011056)
30. Lightfoot JW *et al*. 2021 Sex or cannibalism: polyphenism and kin recognition control social action strategies in nematodes. *Sci. Adv*. **7**, eabg8042. (doi:10.1126/sciadv.abg8042)
31. Cunha TJ, de Medeiros BAS, Lord A, Sørensen MV, Giribet G. 2023 Rampant loss of universal metazoan genes revealed by a chromosome-level genome assembly of the parasitic Nematomorpha. *Curr. Biol*. **33**, 3514–3521. (doi:10.1016/j.cub.2023.07.003)
32. Eleftheriadi K, Guiglielmoni N, Salces-Ortiz J, Vargas-Chavez C, Martínez-Redondo GI, Gut M, Flot JF, Schmidt-Rhaesa A, Fernández R. 2024 The genome sequence of the Montseny horsehair worm, *Gordionus montsenyensis* sp. nov., a key resource to investigate Ecdysozoa evolution. *Peer Community J*. **4**. (doi:10.24072/pcjournal.381)
33. Schmidt-Rhaesa A, Thomas F, Poulin R. 2000 Redescription of *Gordius paranensis* Camerano, 1892 (Nematomorpha), a species new for New Zealand. *J. Nat. Hist*. **34**, 333–340. (doi:10.1080/002229300299516)
34. Gemmell NJ, Akiyama S. 1996 An efficient method for the extraction of DNA from vertebrate tissues. *Trends Genet*. **12**, 338–339. (doi:10.1016/s0168-9525(96)80005-9)
35. Doherty JF, Bhattarai UR, Ferreira S, Poulin R, Gemmell NJ, Dowle EJ. 2023 The proof is in the poo: non-invasive method to detect endoparasitic infection. *Mol. Ecol. Resour*. **23**, 990–1001. (doi:10.1111/1755-0998.13763)
36. Sayers EW *et al*. 2021 Database resources of the national center for biotechnology information. *Nucleic Acids Res*. **50**, D20–D26. (doi:10.1093/nar/gkp382)
37. Weisenfeld NI, Kumar V, Shah P, Church DM, Jaffe DB. 2017 Direct determination of diploid genome sequences. *Genome Res*. **27**, 757–767. (doi:10.1101/gr.214874.116)
38. Kolmogorov M, Yuan J, Lin Y, Pevzner PA. 2019 Assembly of long, error-prone reads using repeat graphs. *Nat. Biotechnol*. **37**, 540–546. (doi:10.1038/s41587-019-0072-8)
39. Simão FA, Waterhouse RM, Ioannidis P, Kriventseva EV, Zdobnov EM. 2015 BUSCO: assessing genome assembly and annotation completeness with single-copy orthologs. *Bioinformatics* **31**, 3210–3212. (doi:10.1093/bioinformatics/btv351)
40. Huang N, Li H. 2023 compleasm: a faster and more accurate reimplementation of BUSCO. *Bioinformatics* **39**, btad595. (doi:10.1093/bioinformatics/btad595)
41. Gurevich A, Saveliev V, Vyahhi N, Tesler G. 2013 QUAST: quality assessment tool for genome assemblies. *Bioinformatics* **29**, 1072–1075. (doi:10.1093/bioinformatics/btt086)
42. Bolger AM, Lohse M, Usadel B. 2014 Trimmomatic: a flexible trimmer for Illumina sequence data. *Bioinformatics* **30**, 2114–2120. (doi:10.1093/bioinformatics/btu170)
43. Kokot M, Długosz M, Deorowicz S. 2017 KMC 3: counting and manipulating *k* -mer statistics. *Bioinformatics* **33**, 2759–2761. (doi:10.1093/bioinformatics/btx304)
44. Ranallo-Benavidez TR, Jaron KS, Schatz MC. 2020 GenomeScope 2.0 and Smudgeplot for reference-free profiling of polyploid genomes. *Nat. Commun*. **11**, 1432. (doi:10.1038/s41467-020-14998-3)
45. Leger A, Leonardi T. 2019 pycoQC, interactive quality control for Oxford Nanopore sequencing. *J. Open Source Softw*. **4**, 1236. (doi:10.21105/joss.01236)
46. Roach MJ, Schmidt SA, Borneman AR. 2018 Purge Haplotigs: allelic contig reassignment for third-gen diploid genome assemblies. *BMC Bioinform*. **19**, 460. (doi:10.1186/s12859-018-2485-7)
47. Jackman SD *et al*. 2018 Tigmint: correcting assembly errors using linked reads from large molecules. *BMC Bioinform*. **19**, 393. (doi:10.1186/s12859-018-2425-6)
48. Dobin A, Davis CA, Schlesinger F, Drenkow J, Zaleski C, Jha S, Batut P, Chaisson M, Gingeras TR. 2013 STAR: ultrafast universal RNA-seq aligner. *Bioinformatics* **29**, 15–21. (doi:10.1093/bioinformatics/bts635)

49. Challis R, Richards E, Rajan J, Cochrane G, Blaxter M. 2020 BlobToolKit – interactive quality assessment of genome assemblies. *G3 Genes Genomes Genetics* **10**, 1361–1374. (doi:10.1534/g3.119.400908)
50. Warren RL. 2016 RAILS and cobbler: scaffolding and automated finishing of draft genomes using long DNA sequences. *J. Open Source Softw*. **1**, 116. (doi:10.21105/joss.00116)
51. Alonge M *et al*. 2022 Automated assembly scaffolding using RagTag elevates a new tomato system for high-throughput genome editing. *Genome Biol*. **23**, 258. (doi:10.1186/s13059-022-02823-7)
52. Baril T, Galbraith J, Hayward A. 2024 Earl Grey: a fully automated user-friendly transposable element annotation and analysis pipeline. *Mol. Biol. Evol.* **41**, msae068. (doi:10.1093/molbev/msae068)
53. Gabriel L, Brůna T, Hoff KJ, Ebel M, Lomsadze A, Borodovsky M, Stanke M. 2024 BRAKER3: fully automated genome annotation using RNA-seq and protein evidence with GeneMark-ETP, AUGUSTUS, and TSEBRA. *bioRxiv,* 2023.2006.2010.544449. (doi:10.1101/2023.06.10.544449)
54. Gabriel L, Hoff KJ, Brůna T, Borodovsky M, Stanke M. 2021 TSEBRA: transcript selector for BRAKER. *BMC Bioinform*. **22**, 566. (doi:10.1186/s12859-021-04482-0)
55. Stanke M, Keller O, Gunduz I, Hayes A, Waack S, Morgenstern B. 2006 AUGUSTUS: ab initio prediction of alternative transcripts. *Nucleic Acids Res*. **34**, W435–W439. (doi:10.1093/nar/gkl200)
56. Camacho C, Coulouris G, Avagyan V, Ma N, Papadopoulos J, Bealer K, Madden TL. 2009 BLAST+: architecture and applications. *BMC Bioinform*. **10**, 421. (doi:10.1186/1471-2105-10-421)
57. Grabherr MG. Trinity: reconstructing a full-length transcriptome without a genome from RNA-Seq data. *Nat. Biotechnol*. **29**, 644–652. (doi:10.1038/nbt.1883)
58. Rochette NC, Rivera-Colón AG, Catchen JM. 2019 Stacks 2: analytical methods for paired-end sequencing improve RADseq-based population genomics. *Mol. Ecol*. **28**, 4737–4754. (doi:10.1111/mec.15253)
59. Li H, Durbin R. 2009 Fast and accurate short read alignment with Burrows–Wheeler transform. *Bioinformatics* **25**, 1754–1760. (doi:10.1093/bioinformatics/btp324)
60. Korneliussen TS, Albrechtsen A, Nielsen R. 2014 ANGSD: analysis of next generation sequencing data. *BMC Bioinform*. **15**, 356. (doi:10.1186/s12859-014-0356-4)
61. Korneliussen TS, Moltke I. 2015 NgsRelate: a software tool for estimating pairwise relatedness from next-generation sequencing data. *Bioinformatics* **31**, 4009–4011. (doi:10.1093/bioinformatics/btv509)
62. R Core Team. 2025 *R: a language and environment for statistical computing*. Vienna, Austria: R Foundation for Statistical Computing. See http://www.R-project.org.
63. Thoendel M, Jeraldo P, Greenwood-Quaintance KE, Yao J, Chia N, Hanssen AD, Abdel MP, Patel R. 2017 Impact of contaminating DNA in whole-genome amplification kits used for metagenomic shotgun sequencing for infection diagnosis. *J. Clin. Microbiol*. **55**, 1789–1801. (doi:10.1128/jcm.02402-16)
64. Hanelt B, Janovy Jr J. 2004 Untying a Gordian knot: the domestication and laboratory maintenance of a Gordian worm, *Paragordius varius* (Nematomorpha: Gordiida). *J. Nat. Hist*. **38**, 939–950. (doi:10.1080/0022293021000058718)
65. eddydowle. 2025 Hairworm_genome_and_kinrelationships. GitHub. See https://github.com/eddydowle/Hairworm_genome_and_kinrelationships.
66. Dowle E *et al*. 2025 Genomic insights into kin selection and developmental conflict in co-occurring hairworm parasites [Dataset]. Dryad Digital Repository. (doi:10.5061/dryad.70rxwdcc2)